Check for updates

Through-conjugation of two phosphaalkyne ('C≡P') moieties mediated by a bimetallic scaffold †

Matthew. C. Leech [ID] and Ian R. Crossley [ID] *

Through-conjugation of two phosphaalkyne moieties within an isolable molecule is demonstrated for the first time with the synthesis of [{Ru(dppe)$_2$}$_2${μ-(C≡C)$_2$C$_6$H$_4$-p}(C≡P)$_2$], *via* base-induced desilylation of [{Ru(dppe)$_2$}$_2${μ-(C≡C)$_2$C$_6$H$_4$-p}(η^1-P≡CSiMe$_3$)$_2$]$^{2+}$. The nature of the cyaphide ligands and their influence upon the bimetallic core are studied electrochemically.

Phosphaalkynes (RC≡P)[1] are archetypal models of the phosphorus–carbon analogy,[2] being both isolobal and isoelectronic with alkynes. Though dichotomous in nature – by virtue of the polarity and lone-pair imparted by phosphorus – their chemical analogy to alkynes is well-established, with a prevalence of cycloaddition/oligomerisation reactions, while both η^2-CP (*cf.* alkynes) and η^1-P (*cf.* nitriles, alkynyls) complexes with transition metals are known.[3] Notwithstanding, an enduring omission lies with the incorporation of the discrete 'C≡P' moiety into architectures featuring extended conjugation (*cf.* the prevalence of polyacetylides), a desirable target – particularly from an organometallic standpoint[4] – given extensive interest in acetylenic and phosphorus-containing moieties in the context of developing molecular electronic components.[5–7] Indeed, the conjugation of phosphaalkyne ('C≡P') moieties with other π-systems is limited to the small range of aromatic phosphaalkynes: PhC≡P,[8] 2,6-R-C$_6$H$_3$C≡P (R = Mes, ^{t}Bu),[9] 2,6-R-4-R'-C$_6$H$_2$C≡P (R = ^{t}Bu, R' = OMe, NMe$_2$;[9b] R=R' = ^{t}Bu,[10] CMe$_2$Et[11]) and the putative P≡C–C≡E (E = CH, N,[12a,b] P[12c–e]), which were generated (transiently) and observed in the gas phase. The latter (P≡C–C≡P) is also among a very limited range of compounds to feature two 'C≡P' moieties (Chart 1),[13] and is the sole precedent example for which their mutual conjugation might reasonably be invoked (albeit unstudied).

Though a small number of transition metal complexes featuring *trans*-disposed η^1-phosphaalkynes has been reported,[14]
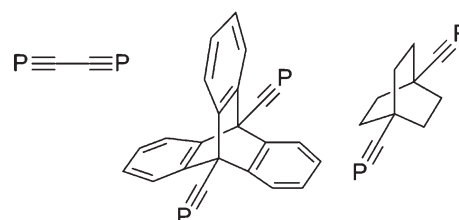
Department of Chemistry, University of Sussex, Brighton, UK.
E-mail: i.crossley@sussex.ac.uk; Fax: +44 (0)1273876678; Tel: +44 (0)1273 877302
†Electronic supplementary information (ESI) available: Synthetic procedures, characterising data and spectra, computational and electrochemical details, orbital plots, X-ray diffraction data. CCDC 1811689. For ESI and crystallographic data in CIF or other electronic format see DOI: 10.1039/c8dt00110c

Chart 1 Known bis-phosphaalkynes.[12,13]

viz. [M(L)$_2$(P≡C^{t}Bu)$_2$] (M = Mo, L = dppe, depe, R$_2$PC$_2$H$_4$PR$_2$, R = Tol, ClC$_6$H$_4$); (M = W, L = dppe), [Mo(depe)$_2$(P≡CAd)$_2$] and [Mo(dppe)$_2$(P≡CSiMe$_3$)$_2$],[15] even the concept of metal-mediated conjugation (*cf.* bis-alkynyl complexes) was unexplored prior to our recent report of the unprecedented cyaphide–alkynyl complexes *trans*-[Ru(dppe)$_2$(C≡CR)(C≡P)] (R = CO$_2$Me, p-An).[16] Herein, we extend this conceptual framework to consider, for the first time, extended conjugation between multiple 'C≡P' moieties, mediated by a bimetallic, redox-active, core; we also elucidate the electronic and redox nature of these complexes.
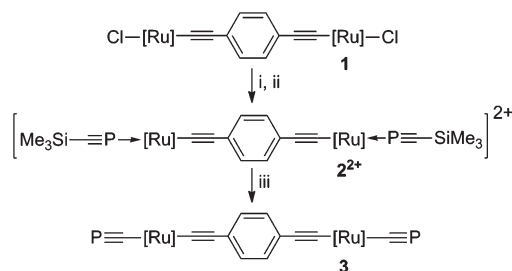
The sequential treatment of the bisethynylbenzene-bridged bimetallic complex [{Ru(dppe)$_2$}$_2${μ-(C≡C)$_2$C$_6$H$_4$-p}Cl$_2$] (**1**) with two equivalents of AgOTf and P≡CSiMe$_3$ facilitates installation of two terminal phosphaalkyne moieties to afford **2^{2+}** (Scheme 1). Formation of **2^{2+}** is evident from characteristic spectroscopic signatures indicative of a coordinated phosphaalkyne (δ_P 111.4, J_{PP} 34 Hz) in proximity to the dppe scaffold (δ_P 42.2 (1:4 ratio)), while the carbon-rich bridge remains apparent from ^{13}C{^{1}H} NMR and infrared ($\nu_{C≡C}$ 2054 cm^{-1}) spectroscopic data. Retention of the silyl moieties follows from heteronuclear (^{1}H–^{29}Si) correlation, while the triflate counter-ion is observed in the ^{19}F-NMR spectrum (δ_F −78.9); bulk composition is affirmed by microanalysis.

The connectivity of **2^{2+}** is further supported by X-ray diffraction data (Fig. 1).[17] The internal geometry is largely unremarkable, exhibiting only slight deviations from linearity about the metal centres (∠ P–Ru–C 173.4(2), 175.3(2)°) and in the bridge

Cl—[Ru]≡≡⟨benzene⟩≡≡[Ru]—Cl **1**

↓ i, ii

[Me₃Si—≡P→[Ru]≡≡⟨benzene⟩≡≡[Ru]←P≡—SiMe₃]²⁺ **2²⁺**

↓ iii

P≡—[Ru]≡≡⟨benzene⟩≡≡[Ru]—≡P **3**

Scheme 1 Reagents and conditions: (i) CH₂Cl₂, 2 AgOTf, (ii) 2 P≡CSiMe₃ in toluene, 1 h.; (iii) thf, 2 KOᵗBu, 1 h. [Ru] = Ru(dppe)₂.

Table 1 Comparative experimental and calculated NMR spectroscopic data[a]

	$\delta_{P(CP)}$	$\Delta\delta_{P(CP)}$[b]	$\delta_{C(CP)}$	$\Delta\delta_{C(CP)}$[b]
2²⁺	111.4	—	189.8	—
3	159.7	48.3	281.8	92.0
[{Ru}(C₂R)(P≡CSiMe₃)]⁺	108.4	—	192.6	—
[{Ru}(C₂R)(C≡P)] (R = CO₂Me)	168.5	60.0	279.1	86.5
[{Ru}(C₂R)(P≡CSiMe₃)]⁺	112.8	—	188.2	—
[{Ru}(C₂R)(C≡P)] (R = p-An)	159.5	46.7	281.9	93.7
[{Ru}H(P≡CSiPh₃)]⁺ ²⁰ᵃ	143.8[c]	—	175.1	—
[{Ru}H(C≡P)]²⁰ᵃ	165.0	21.3	287.1	112.0
2²⁺ (calc)[d]	118.4	—	188.8	—
3 (calc)[d]	166.4	48.0	271.4	82.6

[a] {Ru} = Ru(dppe)₂. [b] $\Delta\delta$ on conversion from η^1-P≡CR to terminal cyaphide. [c] Increase in δ_P due to SiPh₃ vs. SiMe₃. [d] GIAO method with the PBE functional (lanl2dz for Ru; 6-31G** for all other atoms); referenced to H₃PO₄ or Me₄Si at the same level of theory.
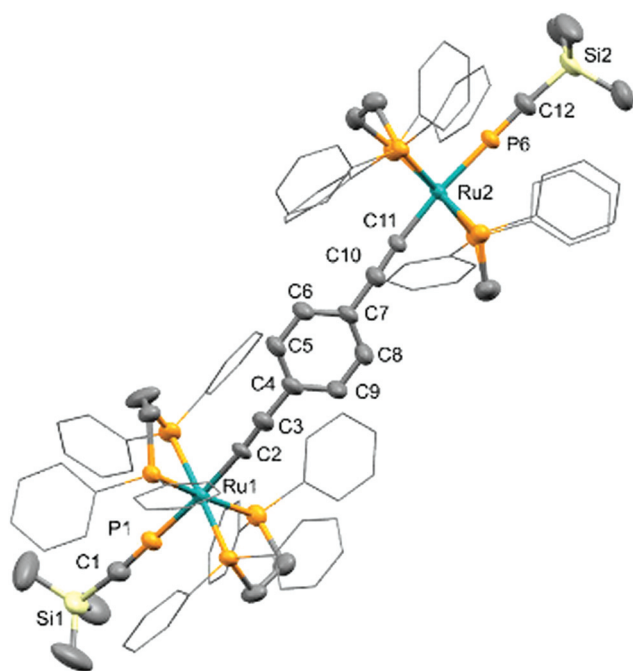

Fig. 1 Molecular structure of **2²⁺**; 50% thermal ellipsoids, hydrogen atoms omitted, and phenyl rings reduced for clarity. Selected bond distances (Å) and angles (°): Ru1–P1 2.264(1), Ru1–C2 2.035(4), Ru2–P6 2.269(1), Ru1–C11 2.022(4), P1–C1 1.526(5), C2–C3 1.203(6), C3–C4 1.443(6)m P6–C12 1.526(5), C10–C11 1.214(6), C10–C7 1.441(6); P1–Ru1–C2 175.23(13), P6–Ru2–C11 173.38(12), C1–P1–Ru1 179.3(2), C12–P6–Ru2 177.3(2), Ru1–C2–C3 174.2(4), Ru2–C11–C10 174.5(4), C2–C3–C4 171.7(5), C11–C10–C7 174.8(5).

(∠ Ru–C≡C 174.5(4), 174.2(4); ∠ C≡C–C 174.5(5), 172.7(5)°) characteristic, respectively, of other bis-alkynyls[18] and the limited range of structurally characterized complexes comprising the 'Ru₂{μ-(C≡C)₂C₆H₄-p}' and related cores.[19] The co-ordinated phosphaalkyne moieties are similarly consistent with related analogues.[14–16,20]

Conversion of the η^1-P≡CSiMe₃ moieties to terminal cyaphide ligands ('–C≡P') proceeds upon treating **2²⁺** with 2 equiv. KOᵗBu,[21] affording **3** in moderate yield (Scheme 1). While single crystals of **3** can be grown, their rapid desolvation during mounting (even at low temperature) has precluded the

acquisition of X-ray diffraction data. Nonetheless, the identity of **3** is readily established from the characteristic spectroscopic features and changes that accompany the desilylative rearrangement of η^1-P≡CSiMe₃ to cyaphide;[16,20a] *viz.* (i) reduction in frequency of the C≡P stretch ($\Delta\nu_{C≡P}$ ~ −12 cm⁻¹); (ii) loss of NMR resonances for silyl and ⁻OTf moieties; (iii) increase in frequency ($\Delta\delta_P$ 48) for the phosphaalkynic P-centres, with reduced magnitude of the P_{CP}–P_{dppe} coupling (precluding its resolution); (iv) increased frequency ($\Delta\delta_c$ 92) for the cyaphidic carbon resonance, consistent with formation of an organometallic linkage (*cf* M–CO, M–CN). These data compare well with those we have noted previously[16] and those for Grutzmacher's seminal complex [RuH(dppe)₂(C≡P)];[20a] they also concur with data calculated for **3** using the PBE functional (Table 1).

The optimized gas-phase geometries of **2²⁺** and **3** (see ESI†)[22] both exhibit slightly greater linearity about the metal centres and bridge when compared with the solid-state structure of **2²⁺**, alongside marginally longer C≡P linkages (~1.58 Å). These features are consistent with a prevalence of packing effects in the solid state, as noted previously for several η^1-P≡CR complexes,[20,23] and for our precedent cyaphide–alkynyls.[16] The calculated C≡P stretching mode for **3** (asym. $\nu_{C≡P}$ 1224 cm⁻¹) also compares well with experiment ($\nu_{C≡P}$ 1247 cm⁻¹). Notably, the experimentally observed frequency reflects a slightly stronger C≡P linkage for **3** than in [RuH(dppe)₂(C≡P)] ($\nu_{C≡P}$ 1239 cm⁻¹),[20a] attributable to competition with the *trans*-alkynyl for Ru → π* donation. Indeed, we noted this previously for cyaphide–alkynyls, though to a greater extent ($\nu_{C≡P}$ 1255, 1260 cm⁻¹),[16] suggesting a reduced competition within the bimetallic scaffold.

The frontier orbitals of **2²⁺** and **3** (Fig. 2) show similarities, the HOMO in each case being dominated by the bridging π-system (76%, **2²⁺**; 54% **3**) with a modest contribution from the metals (14% **2²⁺**; 26% **3**). Notably, the HOMO of **3** also includes contributions from π_{C≡P} (14%), which engage in out-of-phase mixing with the Ru (d_{xy}, d_{xz}), π_{C≡C} and π_{Ar} orbitals, consistent with some level of through-conjugation. The contri-

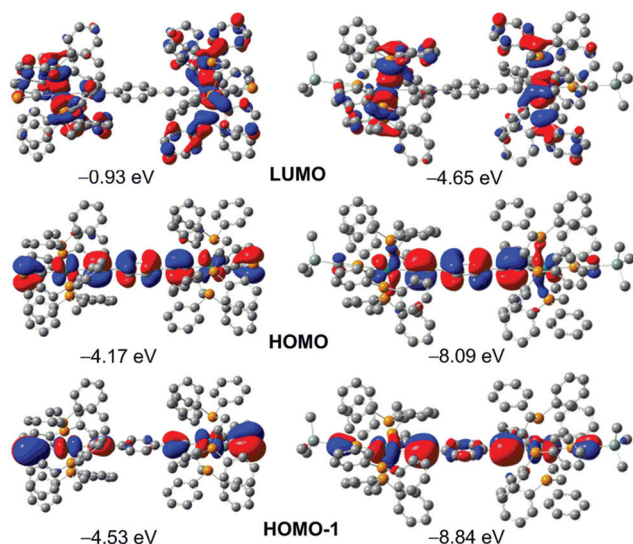**Fig. 2** Frontier orbitals for **3** (left) and **2^{2+}** (right), with relative energies (see also ESI†).

Table 2 Electrochemical (CV) data and comproportionation constants^{a,b}

	E_{pa}/V	E_{pc}/V	$E_{1/2}(\Delta E_{pp})$/V	ΔE_{pa}/V	$K_c{}^b$
1	−0.268	−0.348	−0.308 (80)	0.351	8.9×10^5
	0.081	0.004	0.043 (77)		
2^{2+}	0.705	0.565	0.635 (140)	0.290	0.8×10^5
	0.995				
3	−0.210^c	−0.780^d	—	0.190	1.7×10^3
	−0.020^c				

^{a} CH$_2$Cl$_2$/0.1 M [NBu$_4$]PF$_6$ using 1 mM analyte solutions at (25 °C), with Pt disc (1 mm) working electrode, Pt wire counter electrode and Ag wire pseudo-reference at 100 mV s^{-1}. Potentials relative to the FcH/FcH$^+$ couple (0.00 V), referenced using internal Fc*H/Fc*H$^+$ (−0.56 V (E_{pp} 78 mV) *vs.* Fc/Fc$^+$). ^{b} $K_c = 10^{\Delta E/59 \text{ mV}}$ at 298 K. ^{c} Irreversible oxidation. ^{d} Irreversible reduction.

butions from $\pi_{C\equiv P}$ increase appreciably in the mutually degenerate HOMO−1 and HOMO−2 (~25%, see ESI†), lying 0.36 eV below the HOMO, albeit without involvement of the bridging arene (1%). In marked contrast, there is negligible contribution (<10%) from the η^1-P≡CSiMe$_3$ moieties of **2^{2+}** to any occupied frontier orbitals, their involvement becoming significant only in the appreciably stabilized HOMO−3 and HOMO−4, lying *ca.* 1.4 eV below the HOMO. Finally, in respect of **3**, we note that the terminal cyaphidic lone-pairs manifest in the HOMO−14 and HOMO−15, being stabilised by *ca.* 2 eV relative to the HOMO. This is entirely consistent with expectation, being similar to our previous observations,[16] and those for phosphaalkynes more generally.[24] Additionally, NBO calculations suggest these to reside in orbitals of *ca.* 75% *s* and 25% *p* character, as is typical of phosphaalkynes.

As is typical of complexes with the Ru(dppe)$_2$ scaffold, the latter dominates the virtual orbitals of **3**, which are mostly centred on the dppe ligands; the bridge contributes marginally to LUMO+12 and LUMO+14, lying 4 eV above the HOMO. In contrast, while the LUMO/LUMO+1 of **2^{2+}** are again dominated by the Ru(dppe)$_2$ framework, LUMO+2 is centred on the unsaturated core, with appreciable contributions from $\pi^*_{C\equiv P}$ (60%) and the bridge (15%). This is reflected in the electronic spectrum of **2^{2+}**, assigned in comparison with those derived from TD-DFT studies,[25] calculating the first 200 excited states. This offers a fair approximation of the observed UV spectra for **2^{2+}** and **3** (within limitations of the model), providing sufficient correlation to assist in the assignment of some key features. Thus, a feature at 350 nm (28 571 cm^{-1}) includes significant contribution from LLCT bands ($\pi_{C\equiv C} \to \pi^*_{Ar}$ and $\pi_{C\equiv C} \to \pi^*_{C\equiv P}$) with marginal involvement of intraligand CT ($\pi_{C\equiv C} \to \pi^*_{C\equiv C}$), alongside the dominant MLCT and LLCT associated with excitation from the HOMO/HOMO+1 to low-lying dppe-based orbitals. A second feature around 260 nm (38 462 cm^{-1}) is

primarily composed of ILCT within the dppe scaffold (<HOMO−10 → LUMO), but with additional contribution from $\pi_{C\equiv P} \to \pi^*_{C\equiv P}$ ILCT and $\pi_{Ar} \to \pi^*_{C\equiv P}$ LLCT (HOMO−3 → LUMO+5). In contrast, features in the UV/Vis spectrum of **3** around 370 nm (27 027 cm^{-1}) and 250 nm (40 000 cm^{-1}) are wholly dominated by MLCT and LLCT transitions to the dppe scaffold, with marginal contributions from ILCT within the bridging π-framework; contributions from transitions to the high-lying $\pi^*_{C\equiv P}$ (LUMO+36 to LUMO+39) are negligible.

The redox behaviours of **2^{2+}** and **3** were explored using cyclic voltammetry (Table 2 and ESI†), both compounds exhibiting two distinct oxidative events, which can be assigned (trivially[26]) to sequential generation of the Ru^{III}/Ru^{II} and Ru^{III}/Ru^{III} species. For **2^{2+}** an initial quasi-reversible oxidation occurs at significantly more anodic potential than the corresponding (reversible) feature of **1**, presumably a corollary of its cationic nature. The second (irreversible) oxidation is similarly shifted to more positive potential,[27] and demonstrates an appreciable stability for the mixed valence state [**2^{2+}**]$^+$, K_c being comparable in magnitude to that of [**1**]$^+$ and related terminal alkynyls.[19e,28]

In the case of **3**, two irreversible oxidations are observed, the initial event showing a slight anodic shift relative to **1**, and indeed related alkynyl systems;[19e,28] the second occurs at lower potential than the corresponding oxidation of [**1**]$^+$. On the reverse scan, an irreversible reduction process is observed at heavily cathodic potential. Notably, the diminished separation of the oxidative events indicates a reduced stability for the mixed valence state ([**3**]$^+$) in comparison to [**1**]$^+$ and, indeed, related alkynyl complexes and [**2^{2+}**]$^+$, K_c being two-orders of magnitude lower than for its counterparts.[19e,28] Notwithstanding, some stability is apparent, which implies some retention of the electronic coupling characteristic of the "Ru$_2${μ-(C≡C)$_2$C$_6$H$_4$-*p*}" scaffold, albeit diminished by the seemingly electron-acceptor character of the cyaphide ligand.

Conclusions

In conclusion, we have described the first isolable compound to incorporate two 'C≡P' moieties as part of the same conju-

gated scaffold, *viz.* [Ru$_2${μ-(C≡C)$_2$C$_6$H$_4$-*p*}(C≡P)$_2$] (**3**). The electronic spectrum shows a dominance of LLCT and MLCT transitions from the bridge and phosphacarbon moieties to the dppe scaffold, with negligible ILCT within the π-system. The redox properties of **3** are more interesting and suggest some electron-acceptor character for the cyaphide ligand. While its presence leads to irreversible redox behaviour and serves to destabilize the mixed-valent state [**3**]$^+$, the retention of electronic coupling within the bimetallic core provides initial conceptual validation for the incorporation of the cyaphide ligand into electro-active complexes. This will require engineering of appropriately stabilizing ancillary scaffolds, a challenge with which we are currently engaged.

Conflicts of interest

There are no conflicts to declare.

Acknowledgements

Notes and references

1 For reviews of phosphacarbon and phosphaalkene chemistry see: (*a*) F. Mathey, *Angew. Chem., Int. Ed.*, 2003, **42**, 1578–1604; (*b*) R. Appel, in *Multiple Bonds and Low Coordination in Phosphorus Chemistry*, ed. M. Regitz and O. J. Scherer, Thieme, Stutgart, 1990; (*c*) L. N. Markovski and V. D. Romanenko, *Tetrahedron*, 1989, **45**, 6019–6090; (*d*) R. Appel, F. Knoll and I. Ruppert, *Angew. Chem., Int. Ed. Engl.*, 1981, **20**, 731–744.

2 K. B. Dillon, F. Mathey and J. F. Nixon, *Phosphorus: The Carbon Copy*, Wiley, Chichester, 1998.

3 (*a*) J. F. Nixon, *Coord. Chem. Rev.*, 1995, **145**, 201–258; (*b*) J. F. Nixon, *Chem. Rev.*, 1988, **88**, 1327–1362.

4 See for example and reviews: (*a*) C. Schubert, J. T. Margrat, T. Clark and D. M. Guidi, *Chem. Soc. Rev.*, 2015, **44**, 988–998; (*b*) P. J. Low, *Dalton Trans.*, 2005, 2821–2824; (*c*) M. I. Bruce and P. J. Low, *Adv. Organomet. Chem.*, 2004, **51**, 179–444; (*d*) M. I. Bruce and P. J. Low, *Adv. Organomet. Chem.*, 2001, **48**, 71–288; (*e*) F. Paul and C. Lapinte, *Coord. Chem. Rev.*, 1998, **178–180**, 431–509; (*f*) I. R. Whittall, A. J. McDonagh and M. G. Humphrey, *Adv. Organomet. Chem.*, 1998, **42**, 291–362; (*g*) N. J. Long, *Angew. Chem., Int. Ed. Engl.*, 1995, **34**, 21–38.

5 (*a*) M. A. Shameem and A. Orthaber, *Chem. – Eur. J.*, 2016, **22**, 10718–10735; (*b*) T. Baumgartner, *Acc. Chem. Res.*, 2014,

47, 1613–1622; (*c*) T. Baumgartner and R. Reau, *Chem. Rev.*, 2006, **106**, 4681–4727 and references therein.

6 (*a*) X.-L. Geng, Q. Hu, B. Schafer and S. Ott, *Org. Lett.*, 2010, **12**, 692–695; (*b*) E. Oberg, B. Schafer, X.-L. Geng, J. Pettersson, Q. Hu, M. Kritikos, T. Rasmussen and S. Ott, *J. Org. Chem.*, 2009, **74**, 9265–9273; (*c*) B. Schafer, E. Oberg, M. Kritikoz and S. Ott, *Angew. Chem., Int. Ed.*, 2008, **47**, 8228–8231; (*d*) V. A. Wright, B. O. Patrick, C. Schneider and D. P. Gates, *J. Am. Chem. Soc.*, 2006, **126**, 8836–8844; (*e*) C.-W. Tsang, B. Baharloo, D. Riendi, M. Yam and D. P. Gates, *Angew. Chem., Int. Ed.*, 2004, **43**, 5682–5685; (*f*) C.-W. Tsang, M. Yam and D. P. Gates, *J. Am. Chem. Soc.*, 2003, **125**, 1480–1481.

7 (*a*) X. He, J. Borau-Garcia, A. Y. Y. Woo, S. Trudel and T. Baumgartner, *J. Am. Chem. Soc.*, 2013, **135**, 1137–1147; (*b*) Y. Ren and T. Baumgartner, *Dalton Trans.*, 2012, **41**, 7792–7800; (*c*) P.-A. Bouit, A. Escande, R. Szucs, D. Szieberth, C. Lescop, L. Nyulaszi, M. Hissler and R. Reau, *J. Am. Chem. Soc.*, 2012, **134**, 6524–6527; (*d*) A. Bruch, A. Fukazawa, E. Yamaguchi, S. Yamaguchi and A. Studer, *Angew. Chem., Int. Ed.*, 2011, **50**, 12094–12098.

8 (*a*) C. Mueller, R. Bartsch, A. Fischer, P. G. Jones and R. Schmutzler, *J. Organomet. Chem.*, 1996, **512**, 141–148; (*b*) R. Appel, G. Maier, H. P. Reisenauer and A. Westerhaus, *Angew. Chem., Int. Ed. Engl.*, 1981, **20**, 197–197.

9 (*a*) C. Jones and M. Waugh, *J. Organomet. Chem.*, 2007, **692**, 5086–5090; (*b*) K. Toyota, S. Kawasaki and M. Yoshifuji, *J. Org. Chem.*, 2004, **69**, 5065–5070.

10 (*a*) A. S. Ionkin, W. J. Marshall, B. M. Fish, A. A. Marchione, L. A. Howe, F. Davidson and C. N. McEwen, *Eur. J. Inorg. Chem.*, 2008, 2386–2390; (*b*) G. Markl and H. Sejpka, *Tetrahedron Lett.*, 1986, **27**, 171–174.

11 M. Yoshifuji, H. Kawanami, Y. Kawai, K. Toyota, M. Yasunami, T. Niitsu and N. Inamoto, *Chem. Lett.*, 1992, **21**, 1053–1056.

12 (*a*) T. A. Cooper, H. W. Kroto, J. F. Nixon and O. Ohashi, *J. Chem Soc., Chem. Commun.*, 1980, 333–334; (*b*) H. W. Kroto, J. F. Nixon and K. Ohno, *J. Mol. Spectrosc.*, 1981, **90**, 512–516; (*c*) M. Brönstrup, J. Gottfriedsen, I. Kretzchmar, S. J. Blanksby, H. Schwarz and H. Schumann, *Phys. Chem. Chem. Phys.*, 2000, **2**, 2245–2250; (*d*) L. A. Jones, E. P. F. Lee, P. Soldan and T. G. Wright, *Phys. Chem. Chem. Phys.*, 1999, **1**, 391–395; (*e*) F. M. Bickelhaupt and F. Bickelhaupt, *Chem. – Eur. J.*, 1999, **5**, 162–174.

13 (*a*) F. Brodkorb, M. Brym, C. Jones and C. Schulten, *J. Organomet. Chem.*, 2006, **691**, 1025–1029; (*b*) M. Brym and C. Jones, *Dalton Trans.*, 2003, 3665–3667.

14 P. B. Hitchcock, M. J. Maah, J. F. Nixon, J. A. Zora, G. J. Leigh and M. A. Bakar, *Angew. Chem., Int. Ed. Engl.*, 1987, **26**, 474–475.

15 S. M. Mansell, M. Green and C. A. Russell, *Dalton Trans.*, 2012, **41**, 14360–14368.

16 N. Trathen, M. C. Leech, I. R. Crossley, V. K. Greenacre and S. M. Roe, *Dalton Trans.*, 2014, **43**, 9004–9007.

17 CCDC 1811689† Crystals grown from CH₂Cl₂/hexane at −20 °C. See ESI† for data.

18 (a) M. C. B. Colber, J. Lewis, N. J. Long, P. R. Raithby, A. J. P. White and D. J. Williams, *Dalton Trans.*, 1997, 99–104; (b) N. D. Jones and M. O. Wolf, *Organometallics*, 1997, **16**, 1352–1354; (c) C.-Y. Wong, C.-M. Che, M. C. W. Chan, J. Han, K.-H. Leung, D. L. Phillips, K.-Y. Wong and N. Zhu, *J. Am. Chem. Soc.*, 2005, **127**, 13997–14007; (d) A. Vacher, F. Barriere, T. Roisnel, L. Piekara-Sady and D. Lorcy, *Organometallics*, 2011, **30**, 3570–3578.

19 (a) S. Sporler, L. Muller, A. R. Waterloo, R. R. Tykwinski and N. Burzlaff, *J. Organomet. Chem.*, 2016, **821**, 122–129; (b) X. Wang, X. You, Z.-P. Shang and J. Xia, *J. Organomet. Chem.*, 2016, **803**, 111–118; (c) J. Xia, Y.-P. Ou, D. Wu, G. J. Jin, J. Yin, G.-A. Yu and S. H. Liu, *Dalton Trans.*, 2013, **42**, 14212–14222; (d) M. A. Fox, B. Le Guennic, R. L. Roberts, D. A. Brue, D. S. Yufit, J. A. K. Howard, G. Manca, J.-F. Halet, F. Hartl and P. J. Low, *J. Am. Chem. Soc.*, 2011, **133**, 18433–18446; (e) L. D. Field, A. M. Magill, T. K. Shearer, S. B. Colbran, S. T. Lee, S. J. Dalgarno and M. M. Bhadbhade, *Organometallics*, 2010, **29**, 957–965; (f) D. J. Armitt, M. I. Bruce, M. Gaudio, N. N. Zaitseva, B. W. Skelton, A. H. White, B. L. Guennic, J.-F. Halet, M. A. Fox, R. L. Roberts, F. Harlt and P. J. Low, *Dalton Trans.*, 2008, 6763–6775.

20 (a) J. G. Cordaro, D. Stein, H. Ruegger and H. Grutzmacher, *Angew. Chem., Int. Ed.*, 2006, **45**, 6159–6162; (b) T. Groer, G. Baum and M. Scheer, *Organometallics*, 1998, **17**, 5916–5919.

21 Sub-stoichiometric KO^tBu affords statistical mixture of **2**²⁺ and **3**, with no evidence for the asymmetric (mono-desilylated) product. While separation of the mixture has not been effected, computed NMR data indicate signatures for the asymmetric species to be distinct from those of **2**²⁺ and **3**.

22 Geometries were optimized from an initial model based on the solid state structure of **2**²⁺, using the B3LYP functional (lanl2dz for ruthenium; 6-31G** for all other atoms). See ESI† for full details.

23 C. Jones, C. Schulten and A. Stasch, *Eur. J. Inorg. Chem.*, 2008, 1555–1558.

24 J. C. T. R. Burckett-St. Laurent, M. A. King, H. W. Kroto, J. F. Nixon and R. J. Suffolk, *J. Chem. Soc., Dalton Trans.*, 1983, 755–759.

25 TD-DFT calculations were performed at the B3LYP level using lanl2dz for Ru and 3-21G* for all other atoms, without addition of a solvent model. Though a relatively low level of theory (constituting a balance against the complexity of the system and number of required excited states), such has previously proven suitable to provide a general guide to assignment.

26 Though commonly attributed to sequential Ru^II/Ru^III couples, the oxidation events have heavy involvement from the carbon-rich bridge, due to extensive orbital mixing in the HOMO. These are thus more properly considered as sequential mono-oxidations of the bimetallic core.

27 Though mindful of previous reports of **1** (and related systems) that describe the irreversible oxidation of [**1**]²⁺ close to 1 V,[28b–e] in the present case we are confident in our assignment of this feature to oxidation of the mixed-valence complex [**2**²⁺]⁺ to [**2**²⁺]²⁺, the initial event being more consistent with a 1-electron process.

28 (a) E. Wuttke, Y.-M. Hervault, W. Polit, M. Linseis, P. Erler, S. Rigaut and R. F. Winter, *Organometallics*, 2014, **33**, 4672–4686; (b) A. Benameur, P. Brignou, E. D. Piazza, Y.-M. Hervault, L. Norel and S. Rigaut, *New J. Chem.*, 2011, **35**, 2105–2113; (c) C. Olivier, B. Kim, D. Touchard and S. Rigaut, *Organometallics*, 2008, **27**, 509–518; (d) A. Klein, O. Lavastre and J. Fielder, *Organometallics*, 2006, **25**, 635–643; (e) M. C. B. Colbert, J. Lewis, N. J. Long, P. R. Raithby, M. Younus, A. J. P. White, D. J. Williams, N. N. Payne, L. Yellowlees, D. Beljonne, N. Chawdhury and R. H. Friend, *Organometallics*, 1998, **17**, 3034–3043; (f) S. K. Hurst, M. P. Cifuentes, A. M. McDonagh, M. G. Humphrey, M. Samoc, B. Luther-Davies, I. Asselberghs and A. Persoons, *J. Organomet. Chem.*, 2002, **642**, 250–267; (g) O. Lavastre, J. Plass, P. Bachmann, S. Guesmi, C. Moinet and P. H. Dixneuf, *Organometallics*, 1997, **16**, 184–189.